Electronic Supplementary Material (ESI) for Dalton Transactions


**Supporting Information**

# Micellar self-assemblies of gadolinium(III)/europium(III) amphiphilic complexes as model contrast agents for bimodal imaging

Elke Debroye,[a] Svetlana V. Eliseeva,[b] Sophie Laurent,[c] Luce Vander Elst,[c] Robert N. Muller[c,d] and Tatjana N. Parac-Vogt*[a]

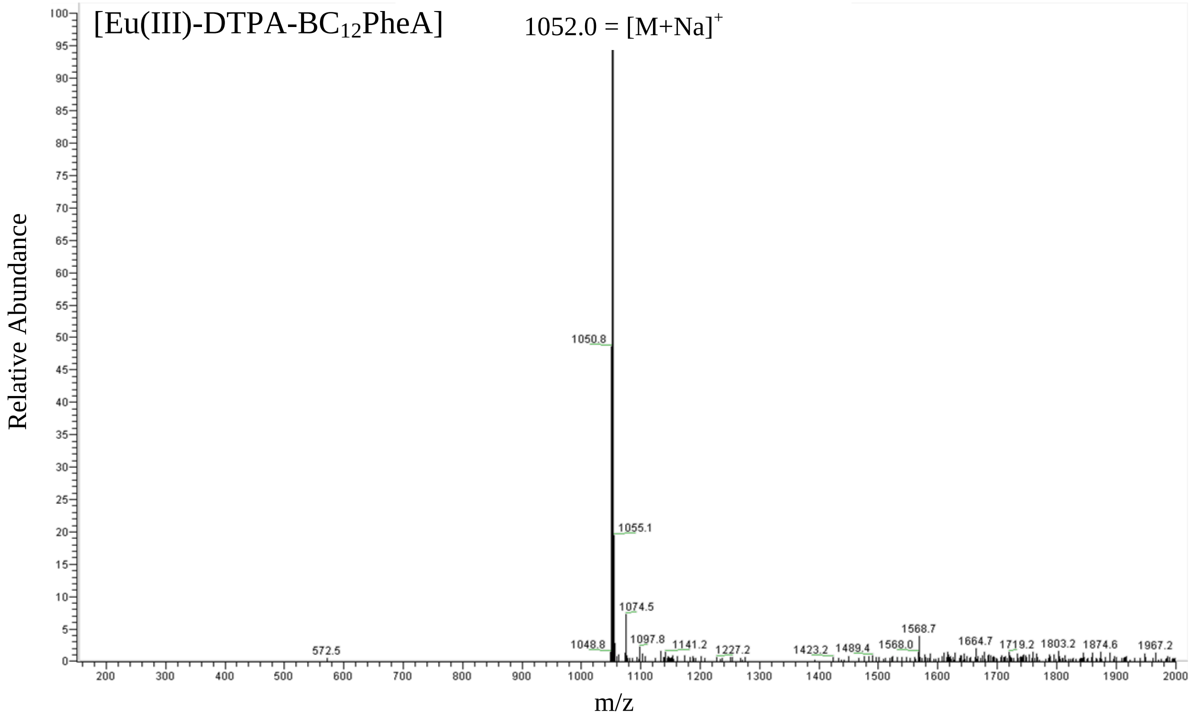


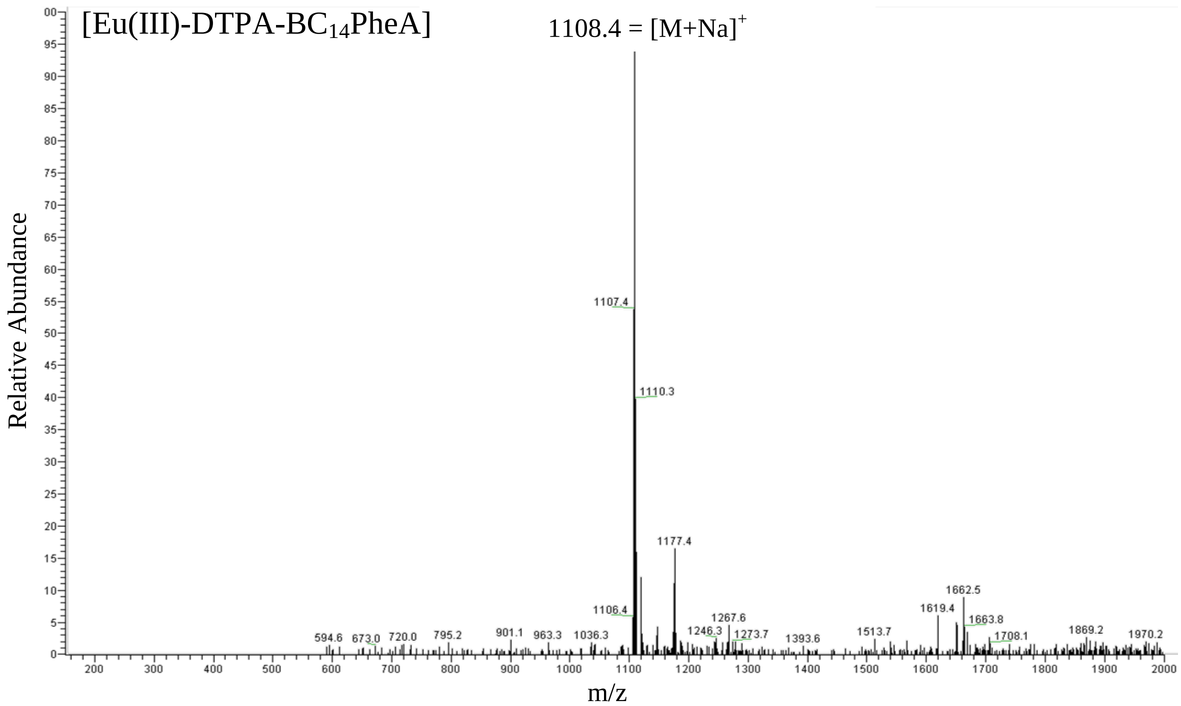


Figure S1. ESI mass spectra of the Eu(III) complexes.

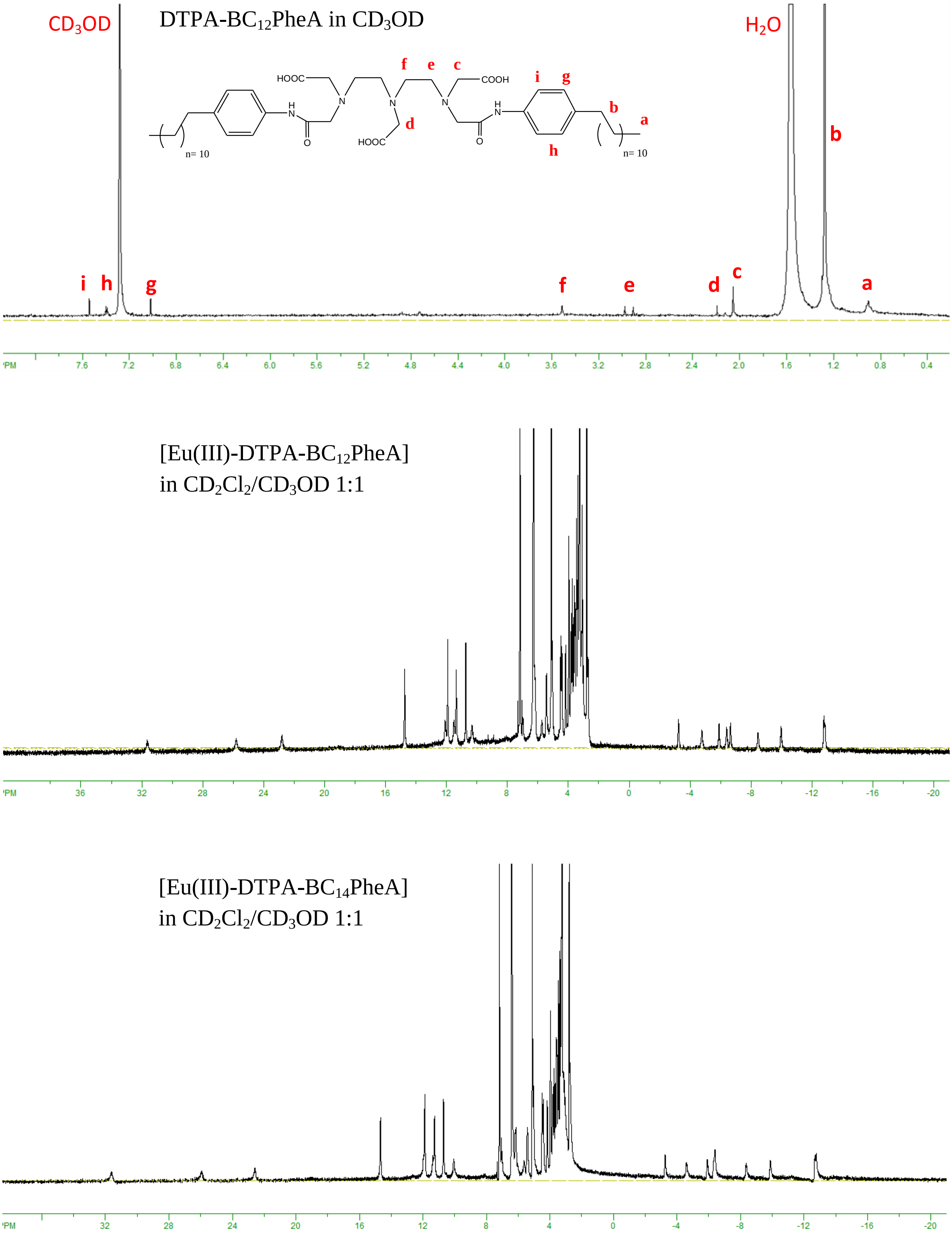


Figure S2. $^{1}H$ NMR spectra of ligand DTPA-$BC_{12}$PheA in $CD_3OD$ and the Ln(III) complexes Eu-DTPA-$BC_{12}$PheA and Eu-DTPA-$BC_{14}$PheA in a 1:1 mixture $CD_2Cl_2/CD_3OD$ (400 MHz, 298 K).

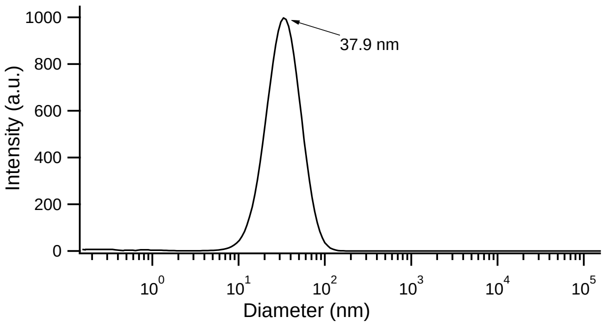


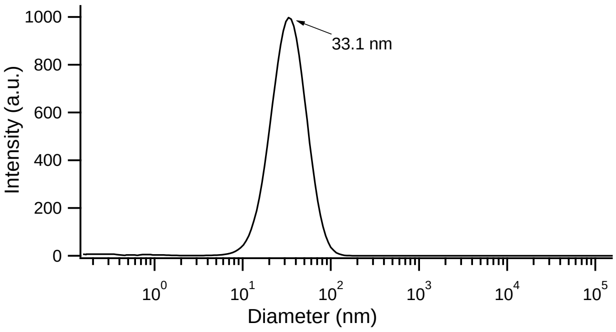


Figure S3. DLS measurements on micelles consisting of Gd(III)/Eu(III)-DTPA-$BC_{12}$PheA (left) and Gd(III)/Eu(III)-DTPA-$BC_{14}$PheA (right) ($H_2O$, $10^{-3}$ M, 298 K).

Table S1.Relative integral intensities of *f*-*f*-transitions for Eu(III) complexes (1:1 $CHCl_3$/MeOH, $10^{-4}$ M, $\lambda_{exc}$ = 290 nm, 298 K).

| $^5D_0 \rightarrow$ | $^7F_0$ | $^7F_1$ | $^7F_2$ | $^7F_3$ | $^7F_4$ | Total |
|---|---|---|---|---|---|---|
| Eu-DTPA-$BC_{12}$PheA | 0.16 | 1.00 | 2.25 | 0.11 | 1.84 | 5.41 |
| Eu-DPTA-$BC_{14}$PheA | 0.14 | 1.00 | 2.42 | 0.10 | 1.96 | 5.72 |

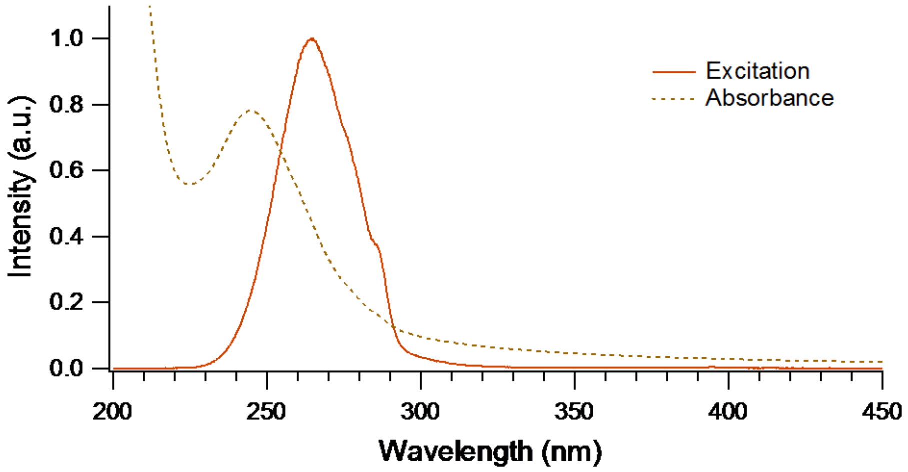


Figure S4. Normalized excitation spectrum (solid trace) and absorption spectrum (dashed trace) of micelles consisting of Eu-DTPA-$BC_{14}$PheA ($H_2O$, $10^{-5}$ M, 298 K).

Table S2. Relative integral intensities of *f*-*f*-transitions for micelles consisting of Eu(III) complexes ($H_2O$, $10^{-4}$ M, $\lambda_{exc}$ = 290 nm, 298 K).

| $^5D_0 \rightarrow$ | $^7F_0$ | $^7F_1$ | $^7F_2$ | $^7F_3$ | $^7F_4$ | Total |
|---|---|---|---|---|---|---|
| Eu-DTPA-$BC_{12}$PheA | 0.15 | 1.00 | 2.75 | 0.06 | 1.46 | 5.42 |
| Eu-DPTA-$BC_{14}$PheA | 0.15 | 1.00 | 2.74 | 0.05 | 1.47 | 5.42 |

Table S3. Photophysical data for micelles consisting of Eu-DTPA-$BC_{12}$PheA and Eu-DTPA-$BC_{14}$PheA in water ($H_2O$, $10^{-4}$ M, $\lambda_{exc}$ = 290 nm, 298 K).

| | $\tau_{H2O}$ (ms) | $\tau_{D2O}$ (ms) | $q_{H2O}$ | $\tau_{rad}$ (ms) | $Q_{Eu}^{Eu}$ (%) | $Q_{Eu}^{L}$ (%) | $\eta_{sens}$ |
|---|---|---|---|---|---|---|---|
| Mic $C_{12}$ | 1.36 (± 0.01) | 2.21 (± 0.02) | 0.1 | 5.24 | 26.0 | 0.98 | 3.8 |
| Mic $C_{14}$ | 1.39 (± 0.01) | 2.19 (± 0.04) | 0.1 | 5.24 | 26.5 | 1.10 | 4.1 |

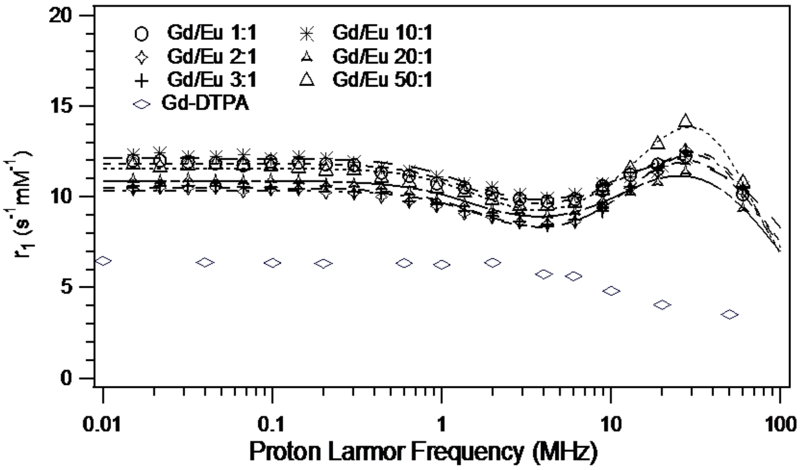


Figure S5. [1]H NMRD profiles of micelles composed of Gd/Eu-DTPA-$BC_{12}$PheA complexes compared to Gd-DTPA in water at 37 °C. The dashed traces represent the fitted data.

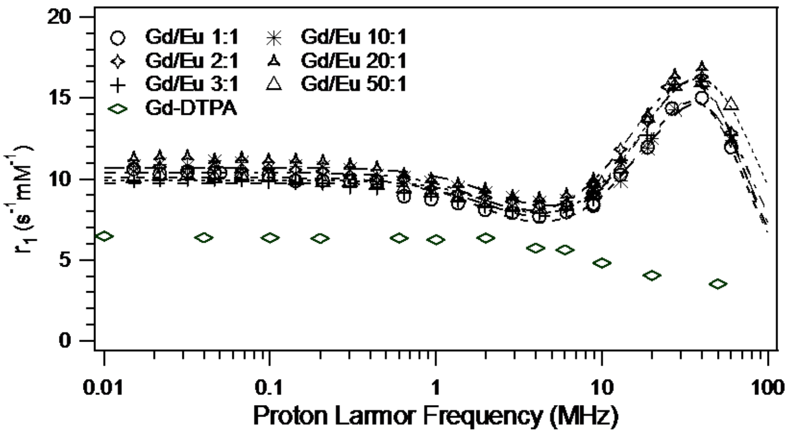


Figure S6. [1]H NMRD profiles of micelles composed of Gd/Eu-DTPA-$BC_{14}$PheA complexes compared to Gd-DTPA in water at 37 °C. The dashed traces represent the fitted data.

Table S4. Parameters obtained by theoretical fitting of the [1]H NMRD data of micelles consisting of Gd/Eu-DTPA-$BC_{12}$PheA (37 °C).

| | **Gd/Eu 1:1** | **Gd/Eu 2:1** | **Gd/Eu 3:1** | **Gd/Eu 10:1** | **Gd/Eu 20:1** | **Gd/Eu 50:1** |
|---|---|---|---|---|---|---|
| $\tau_R$ (ns) | 3.5 ± 0.5 | 4.6 ± 0.8 | 4.4 ± 0.8 | 2.4 ± 0.4 | 3.5 ± 0.6 | 6.5 ± 1.1 |
| $q$ | 0.37 ± 0.01 | 0.41 ± 0.01 | 0.42 ± 0.01 | 0.38 ± 0.01 | 0.34 ± 0.01 | 0.45 ± 0.01 |
| $q_{ss}$ | 2.4 ± 0.3 | 2.5 ± 0.9 | 2.1 ± 0.9 | 2.0 ± 0.2 | 2.0 ± 0.2 | 3.3 ± 1.9 |

| | | | | | | |
|---|---|---|---|---|---|---|
| $\tau_{ss}$ (ps) | 40.1 ± 6.8 | 22.0 ± 8.4 | 26.9 ± 12.9 | 49.5 ± 8.5 | 40.0 ± 1.0 | 21.6 ± 13 |
| $\tau_{SO}$ (ps) | 195 ± 13 | 160 ± 10 | 163 ± 9 | 201 ± 7 | 190 ± 13 | 165 ± 11 |
| $\tau_V$ (ps) | 33.5 ± 1.8 | 27.8 ± 1.9 | 27.6 ± 2.3 | 36.6 ± 2.6 | 33.7 ± 1.4 | 26.9 ± 2.9 |

Table S5. Parameters obtained by theoretical fitting of the $^1$H NMRD data of micelles consisting of Gd/Eu-DTPA-BC$_{14}$PheA (37 °C).

| | Gd/Eu 1:1 | Gd/Eu 2:1 | Gd/Eu 3:1 | Gd/Eu 10:1 | Gd/Eu 20:1 | Gd/Eu 50:1 |
|---|---|---|---|---|---|---|
| $\tau_R$ (ns) | 8.4 ± 1.4 | 6.0 ± 0.9 | 9.2 ± 1.2 | 8.0 ± 2.9 | 3.4 ± 0.7 | 4.3 ± 0.8 |
| $q$ | 0.55 ± 0.01 | 0.59 ± 0.01 | 0.60 ± 0.01 | 0.53 ± 0.01 | 0.58 ± 0.02 | 0.64 ± 0.01 |
| $q_{ss}$ | 1.5 ± 0.5 | 1.3 ± 0.1 | 1.7 ± 0.1 | 3.4 ± 1.7 | 2.6 ± 0.2 | 1.1 ± 0.7 |
| $\tau_{ss}$ (ps) | 10.0 ± 5.8 | 18.7 ± 2.6 | 14.4 ± 0.7 | 17.0 ± 9.0 | 67.0 ± 7.0 | 25.7 ± 7.0 |
| $\tau_{SO}$ (ps) | 147 ± 6 | 136 ± 6 | 116 ± 1 | 125 ± 7 | 88 ± 4 | 111 ± 5 |
| $\tau_V$ (ps) | 21.3 ± 0.5 | 26.8 ± 0.7 | 24.4 ± 0.3 | 21.1 ± 1.6 | 30.1 ± 0.8 | 25.6 ± 1.1 |

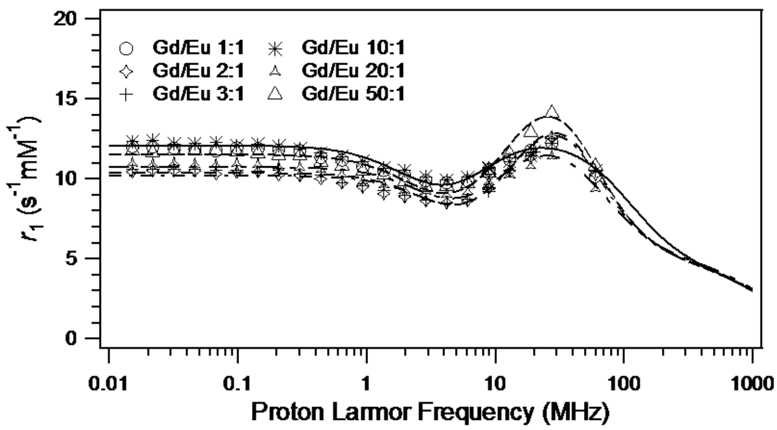


Figure S7. $^1$H NMRD profiles of micelles composed of Gd/Eu-DTPA-BC$_{12}$PheA complexes compared to Gd-DTPA in water at 37 °C. The dashed traces represent the fitted data using the Lipari-Szabo model.

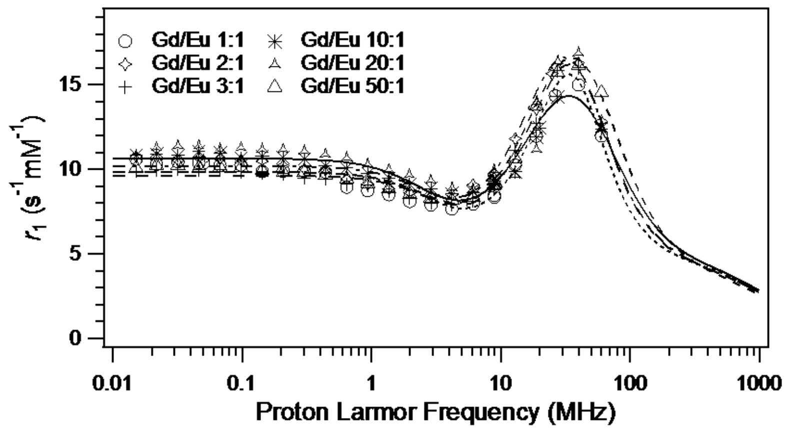


Figure S8. $^1$H NMRD profiles of micelles composed of Gd/Eu-DTPA-BC$_{14}$PheA complexes compared to Gd-DTPA in water at 37 °C. The dashed traces represent the fitted data using the Lipari-Szabo model.

Table S6. Parameters obtained by theoretical fitting of the $^{1}$H NMRD data of micelles consisting of Gd/Eu-DTPA-BC$_{12}$PheA (37 °C) using the Lipari-Szabo model.

| | **Gd/Eu 1:1** | **Gd/Eu 2:1** | **Gd/Eu 3:1** | **Gd/Eu 10:1** | **Gd/Eu 20:1** | **Gd/Eu 50:1** |
|---|---|---|---|---|---|---|
| $\tau_{RG}$ (ns) | 2.2 ± 0.2 | 3.1 ± 0.3 | 3.0 ± 0.3 | 1.5 ± 0.2 | 2.5 ± 0.3 | 3.2 ± 0.3 |
| $\tau_{SO}$ (ps) | 190 ± 4 | 129 ± 2 | 133 ± 2 | 196 ± 6 | 154 ± 3 | 170 ± 3 |
| $\tau_{V}$ (ps) | 49.3 ± 1.7 | 40.0 ± 1.3 | 38.6 ± 1.3 | 50.0 ± 6.6 | 47.6 ± 1.8 | 41.7 ± 1.4 |
| $\tau_{RL}$ (ps) | 150 ± 3 | 150 ± 5 | 150 ± 4 | 150 ± 8 | 150 ± 4 | 150 ± 5 |
| $S^2$ | 0.18 ± 0.02 | 0.18 ± 0.01 | 0.19 ± 0.01 | 0.23 ± 0.03 | 0.15 ± 0.01 | 0.21 ± 0.01 |

Table S7. Parameters obtained by theoretical fitting of the $^{1}$H NMRD data of micelles consisting of Gd/Eu-DTPA-BC$_{14}$PheA (37 °C) using the Lipari-Szabo model.

| | **Gd/Eu 1:1** | **Gd/Eu 2:1** | **Gd/Eu 3:1** | **Gd/Eu 10:1** | **Gd/Eu 20:1** | **Gd/Eu 50:1** |
|---|---|---|---|---|---|---|
| $\tau_{RG}$ (ns) | 6.5 ± 0.9 | 4.4 ± 0.4 | 5.7 ± 0.7 | 2.9 ± 0.3 | 2.1 ± 0.4 | 3.2 ± 0.4 |
| $\tau_{SO}$ (ps) | 108 ± 1 | 114 ± 2 | 101 ± 1 | 131 ± 2 | 127 ± 4 | 102 ± 1 |
| $\tau_{V}$ (ps) | 27.2 ± 0.7 | 33.3 ± 0.6 | 30.4 ± 0.8 | 30.1 ± 1.0 | 33.2 ± 1.0 | 30.2 ± 0.7 |
| $\tau_{RL}$ (ps) | 150 ± 3 | 150 ± 3 | 150 ± 2 | 150 ± 8 | 471 ± 129 | 150 ± 7 |
| $S^2$ | 0.30 ± 0.01 | 0.33 ± 0.01 | 0.34 ± 0.01 | 0.29 ± 0.01 | 0.34 ± 0.09 | 0.41 ± 0.02 |